Monopedal Running Control: SLIP Embedding and Virtual Constraint Controllers

Ioannis Poulakakis, and J. W. Grizzle

Abstract— **Two feedback controllers that induce stable running gaits on a three-degree-of-freedom asymmetric hopper, termed the Asymmetric Spring Loaded Inverted Pendulum (ASLIP), see Fig. 1, are compared in terms of their steady-state and transient behaviors. In each case, feedback is used to create a lower-dimensional hybrid subsystem that determines the existence and stability properties of periodic motions of the full-dimensional closed-loop system. The first controller creates a one degree-of-freedom subsystem through imposing two suitably selected (virtual) holonomic constraints on the configuration variables of the ASLIP. The second controller asymptotically imposes a single (virtual) holonomic constraint to create a two-degree-of-freedom subsystem that is diffeomorphic to a standard Spring Loaded Inverted Pendulum (SLIP). The two controllers induce identical steady-state behaviors. Under transient conditions, however, the underlying compliant nature of the SLIP allows significantly larger disturbances to be accommodated, with less actuator effort, and without violation of the unilateral constraints between the leg end and the ground.**

I. Introduction

The Spring Loaded Inverted Pendulum (SLIP) has proven useful in (qualitatively) explaining various aspects of running in animals [5], and in designing empirical controllers for dynamic legged robots [9], [1]. The success of the SLIP in predicting essential features of sagittal plane running has prompted a further study aimed at understanding whether the SLIP truly represents a dynamic model of running, and thus would be an interesting target model for legged robots, [5], [11]. These research efforts have produced a large variety of controllers for the SLIP; see [11] and references therein, and more recently [12] and [2]. Moreover, these controllers have been employed successfully in the control of multi-legged running [10].

The hybrid dynamics and underactuation inherent in legged locomotion have stymied the formal extension of SLIP controllers to more elaborate models that enjoy a more faithful correspondence to a typical locomotor's structure and morphology. Only a few results are available, including [1] (where experimental results are also provided), and [3], in which controllers for running models that include torso dynamics, energy dissipation and leg inertia exploit results known for the SLIP. However, in all these models the hip joint coincides with the torso center-of -mass (COM), an assumption which is relaxed in this paper.

I. Poulakakis and J. W. Grizzle are with the Control Systems Laboratory, Department of Electrical Engineering and Computer Science, University of Michigan, Ann Arbor, MI 48109, U.S.A. This work was supported by NSF grant ECS 0600869. Email: {poulakas,grizzle}@umich.edu.

Additional results are provided at http://www.eecs.umich.edu/~grizzle/.

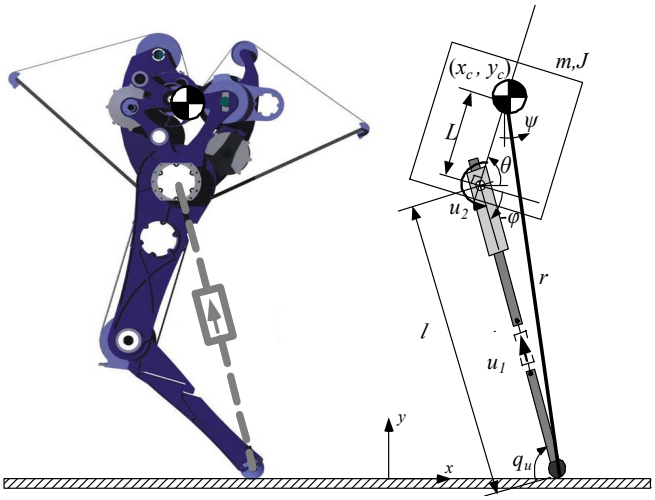

Fig. 1. (Left) A preliminary design of a leg for a bipedal robot that is currently under construction; for the design philosophy and details see [6]. The knee has a revolute series compliant actuator. (Right) The Asymmetric Spring Loaded Inverted Pendulum (ASLIP). The leg force u_1 will be modeled as a spring in parallel with a prismatic force source. The ASLIP is a more faithful representation of the robot on the left than a SLIP model.

A quite different paradigm for control law design has been followed in [13], [4], [7], where geometric nonlinear control methods have been developed that deal directly with the underactuation and hybrid dynamics present in bipedal locomotion. This work has produced feedback controllers that induce *provably*, asymptotically stable, dynamic walking and running motions in a class of planar bipedal robots. In particular, it has been shown that planar walking and running gaits can be "embedded" in the dynamics of a closed-loop system through the creation of a reduced-order *hybrid* subsystem, called the *Hybrid Zero Dynamics (HZD)*.

A drawback of [13] and [4] was that compliance, such as that present in a SLIP model, could not be easily accommodated. This has been overcome in [8], where a more complete SLIP-like model that includes nontrivial pitch dynamics, called the Asymmetric Spring Loaded Inverted Pendulum (ASLIP) (see Fig. 1), was successfully controlled by embedding the SLIP as its HZD.

In this paper, the performance benefits of embedding the SLIP as the HZD of the ASLIP are evaluated by comparing it to a controller design that achieves a one degree-of-freedom (DOF), *non-compliant* HZD. The two controllers induce identical steady-state behaviors. Under transient conditions, however, the underlying compliant nature of the SLIP allows significantly larger disturbances to be accommodated, with less actuator effort, and without

violation of the unilateral toe-ground constraints.

The results presented in this paper provide the first step toward a general framework for the design of control laws that induce elegant, provably stable, running motions in legged robots, by combining the practical advantages of the compliant SLIP with the analytical tractability offered by the HZD method introduced in [13].

II. The Asymmetric Spring Loaded Inverted Pendulum

A schematic for the Asymmetric Spring Loaded Inverted Pendulum (ASLIP) is presented in Fig. 1. The hip joint (point at which the leg is attached to the torso) does not coincide with the COM of the torso, which is modeled as a rigid body with mass m and moment of inertia about the COM J. The leg is assumed to be massless. The ASLIP is actuated with two inputs: a force u_1 acting along the leg, and a torque u_2 applied at the hip. In Section VI, the leg force u_1 will be modeled as a spring in parallel with a prismatic force source. In what follows, the subscripts "f" and "s" denote the flight and stance phases respectively.

A. Flight Phase Dynamics

The flight phase dynamics corresponds to a point mass undergoing ballistic motion in a gravitational field together with a double integrator governing the pitch motion. The configuration space Q_{f} of the flight phase is parameterized by the Cartesian coordinates x_{c} and y_{c} of the COM, together with the pitch angle θ, i.e. $q_{\mathrm{f}} = (x_{\mathrm{c}}, y_{\mathrm{c}}, \theta)' \in Q_{\mathrm{f}}$. The flight phase dynamics can be easily written in state-space form

$$\dot{x}_{\mathrm{f}} = f_{\mathrm{f}}(x_{\mathrm{f}}). \tag{1}$$

The flight phase terminates when the vertical distance of the toe from the ground becomes zero. To realize this condition, the flight state vector is augmented with the touchdown leg length l^{td} and angle φ^{td}, $\alpha_{\mathrm{f}} = (l^{\mathrm{td}}, \varphi^{\mathrm{td}})'$. Since the leg is assumed massless, during flight it obtains the desired length and orientation instantaneously, hence $\dot{\alpha}_{\mathrm{f}} = 0$. The threshold function $H_{\mathrm{f}\to\mathrm{s}}$, whose zero crossing signifies the touchdown event, is given by

$$H_{\mathrm{f}\to\mathrm{s}}(x_{\mathrm{f}}, \alpha_{\mathrm{f}}) = y_{\mathrm{c}} - l^{\mathrm{td}} \cos(\varphi^{\mathrm{td}} + \theta) - L\sin\theta, \tag{2}$$

Note that in (2), the parameter α_{f} is available for control and will eventually be chosen according to an event-based feedback law.

B. Stance Phase Dynamics

The configuration space Q_{s} of the ASLIP during stance is parameterized by $q_{\mathrm{s}} = (l, \varphi, \theta)' \in Q_{\mathrm{s}}$. Using the method of Lagrange and then bringing the equations in standard state-space form, the ASLIP stance dynamics is described by

$$\dot{x}_{\mathrm{s}} = f_{\mathrm{s}}(x_{\mathrm{s}}) + g_{\mathrm{s}}(x_{\mathrm{s}})u, \tag{3}$$

where $x_{\mathrm{s}} = (q_{\mathrm{s}}', \dot{q}_{\mathrm{s}}')'$ is the state vector, and $u = (u_1, u_2)'$ is the input vector during stance. The threshold function, specifying the liftoff event at its zero crossing, is given by

$$H_{\mathrm{s}\to\mathrm{f}}(x_{\mathrm{s}}, u) = u_1 \cos(\varphi+\theta) - (u_2/l)\sin(\varphi+\theta), \tag{4}$$

which describes the fact that liftoff occurs when the vertical component of the ground force becomes zero. Define

$$S_{\mathrm{s}\to\mathrm{f}} = \left\{ (x_{\mathrm{s}}, u) \in TQ_{\mathrm{s}} \times U \,\middle|\, H_{\mathrm{s}\to\mathrm{f}}(x_{\mathrm{s}}, u) = 0 \right\}. \tag{5}$$

C. Open-Loop Hybrid Dynamics

The ASLIP hybrid dynamics, combining the stance and flight phases with the discrete transitions among them, can be compactly written in the form of a system with impulse effects [8]. If Δ is the map taking the state x_{s}^- just prior to liftoff to the state x_{s}^+ just after touchdown, then the ASLIP takes the form

$$\Sigma_{\mathrm{ASLIP}} : \begin{cases} \dot{x}_{\mathrm{s}} = f_{\mathrm{s}}(x_{\mathrm{s}}) + g_{\mathrm{s}}(x_{\mathrm{s}})u, & (x_{\mathrm{s}}^-, u) \notin S_{\mathrm{s}\to\mathrm{f}} \\ x_{\mathrm{s}}^+ = \Delta(x_{\mathrm{s}}^-, u, \alpha_{\mathrm{f}}), & (x_{\mathrm{s}}^-, u) \in S_{\mathrm{s}\to\mathrm{f}} \end{cases}. \tag{6}$$

The map Δ "compresses" the flight phase into an "event," and can be obtained numerically. Equation (6) shows that Σ_{ASLIP} is defined on a single chart TQ_{s}, where the states evolve continuously, together with the map Δ, which reinitializes the differential equation at liftoff.

III. Control Laws: General Development

In this section, the general framework, within which the ASLIP controllers are designed, is outlined. In this paper, rather than concentrating on the theoretical development of the control laws, we turn our attention to design and implementation issues including a comparison of two controllers for the ASLIP constructed along the same general guidelines, which are briefly discussed in this section. Details regarding analytical stability proofs not included in this paper can be found in [13], [7] and [8].

A. Overview of the Control Method

The feedback law exploits the hybrid nature of the system by introducing control action in two levels; see Fig. 2. At the first level, a continuous-time feedback law Γ_{c} is employed in the stance phase with the purpose of creating an invariant and attractive surface Z in the stance state space, on which the dynamics of the ALIP is restricted. At the second level, event-based updates of controller parameters are performed at transitions from stance to flight. Generally, the event-based parameter update law is organized in an inner/outer-loop architecture, with the inner-loop controller Γ_{s} intended to render the surface Z invariant under the reset map Δ. This condition is referred to as *hybrid invariance*, and it leads to the creation of a reduced-order *hybrid* subsystem governing the stability properties of the full-order ASLIP

model, called the *Hybrid Zero Dynamics (HZD)*. In cases where the in-stride (continuous) controller achieves hybrid invariance, Γ_s is not needed and may be excluded from the controller design; see Section V for one such example. Finally, the outer-loop controller Γ_f completes the control design by ensuring that the resulting HZD is exponentially stable.

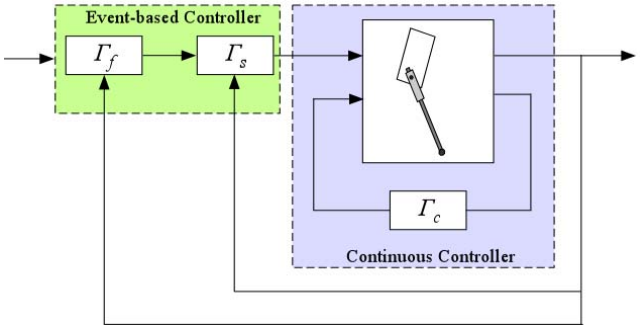

Fig. 2. Feedback diagram presenting the basic structure of the controllers.

In Sections IV and V we particularize these ideas through explicit constructions of two sets of feedback laws Γ_c, Γ_s and Γ_f that achieve the control objectives. In the first case, the control objective during the stance phase is to impose virtual holonomic constraints on the ASLIP dynamics, so that the resulting HZD is a one DOF mechanical system; because the resulting HZD is not compliant, we refer to this controller as the *rigid target model controller*. In the second case, the objective is to achieve a compliant HZD. Based on the extensive literature available on the Spring Loaded Inverted Pendulum (SLIP), see for instance [2], [5], [11], [12], the compliant SLIP is selected as the target model, and a controller is designed that imposes its dynamics as the HZD of the ASLIP; this controller is referred to as the *SLIP embedding controller*, [8]. Fundamental differences in the two control designs will be highlighted in Section VI.

B. In-Stride Continuous Control

To the continuous part of (6), associate the output

$$y = h(q_s, \alpha_s), \tag{7}$$

which depends on the configuration variables q_s, and on a set of parameters $\alpha_s \in A_s$. These parameters can be the coefficients of polynomials representing a set of virtual constraints, or the mechanical properties of a target model, and they remain constant during stance i.e. $\dot{\alpha}_s = 0$.

Given a set of values for the parameters α_s, differentiating (7) twice with respect to time results in

$$\frac{d^2 y}{dt^2} = L_{f_s}^2 h(x_s, \alpha_s) + L_{g_s} L_{f_s} h(q_s, \alpha_s) u, \tag{8}$$

where $L_{g_s} L_{f_s} h(q_s, \alpha_s)$ is the decoupling matrix. Under the condition that $L_{g_s} L_{f_s} h(q_s, \alpha_s)$ is invertible,

$$u^*(x_s, \alpha_s) = -\left(L_{g_s} L_{f_s} h(q_s, \alpha_s)\right)^{-1} L_{f_s}^2 h(x_s, \alpha_s) \tag{9}$$

is the unique control input that renders the surface

$$Z_{\alpha_s} = \left\{ x_s \in TQ_s \,\middle|\, h(q_s, \alpha_s) = 0, L_{f_s} h(x_s, \alpha_s) = 0 \right\} \tag{10}$$

invariant under the flow of the continuous part of the ASLIP dynamics (6); that is, for every $x \in Z_{\alpha_s}$,

$$f^*(x, \alpha_s) = f_s(x) + g_s(x) u^*(x, \alpha_s) \in T_x Z_{\alpha_s}. \tag{11}$$

Following standard terminology, the surface Z_{α_s} is the stance phase zero dynamics manifold, and

$$\dot{z} = f^*|_{Z_{\alpha_s}}(z, \alpha_s) \tag{12}$$

is the stance phase zero dynamics. To establish *attractivity* of Z_{α_s}, the input (9) is modified as

$$\begin{aligned} u &= \Gamma_c(x_s, \alpha_s) \\ &= \left(L_{g_s} L_{f_s} h(q_s, \alpha_s)\right)^{-1} \left[\upsilon(y, \dot{y}, \varepsilon) - L_{f_s}^2 h(x_s, \alpha_s) \right], \end{aligned} \tag{13}$$

where

$$\upsilon(y, \dot{y}, \varepsilon) = -\frac{1}{\varepsilon^2} K_P^y y - \frac{1}{\varepsilon} K_V^y \dot{y}, \tag{14}$$

and K_P^y, K_V^y are appropriately chosen gain matrices, and $\varepsilon > 0$. Under the feedback law Γ_c, the hybrid system (6) takes the form

$$\Sigma_{\text{ASLIP}}^{\text{cl}} : \begin{cases} \dot{x}_s = f_{s,\text{cl}}(x_s, \alpha_s), & x_s^- \notin S_{s\to f} \\ x_s^+ = \Delta(x_s^-, \alpha_f), & x_s^- \in S_{s\to f} \end{cases}, \tag{15}$$

where

$$f_{s,\text{cl}}(x_s, \alpha_s) = f_s(x_s) + g_s(x_s) \Gamma_c(x_s, \alpha_s). \tag{16}$$

C. Event-Based Control

A key implication of the hybrid nature of (15) combined with the (trivial) dynamics $\dot{\alpha}_s = 0$ and $\dot{\alpha}_f = 0$ governing the parameters in (15), is the possibility of updating α_s and α_f in an event-based manner. More specifically, at each crossing of the surface $S_{s\to f}$, α_s and α_f can be updated based on feedback of the liftoff state $x_s^- \in S_{s\to f}$, i.e.

$$\alpha_f = \Gamma_f(x_s^-), \tag{17}$$

$$\alpha_s^+ = \Gamma_s(x_s^-, \alpha_f) = \Gamma_s(x_s^-, \Gamma_f(x_s^-)), \tag{18}$$

with the purpose of the feedback laws Γ_s and Γ_f being to extend the notion of invariance in the hybrid setting, and to ensure stability of the resulting HZD. Loosely speaking, (17) introduces control authority over the initial conditions of the continuous part of (15). On the other hand, (18) allows for "real-time" motion planning in stance via updating α_s.

To ensure hybrid invariance, the inner-loop controller Γ_s is designed to provide updated values α_s^+ of the stance parameters so that the following conditions are satisfied:

(i) the surface $S_{s\to f}\cap Z_{\alpha_s}$, corresponding to those states of Z_{α_s} resulting at liftoff, is the same as $S_{s\to f}\cap Z_{\alpha_s^+}$; denote $S_{s\to f}\cap Z_{\alpha_s}$ by $S_{s\to f}\cap Z_{\blacklozenge}$, and

(ii) $S_{s\to f}\cap Z_{\blacklozenge}$ is invariant under the reset map Δ i.e. $\Delta\big((S_{s\to f}\cap Z_{\blacklozenge})\times A_f\big)\subset Z_{\alpha_s^+}$.

In words, (i) means that liftoff occurs where it would have occurred without updating α_s. Enforcing (i) and (ii) through the update law Γ_s results in the creation of a lower-dimensional *hybrid* subsystem, the HZD, which has the form

$$\Sigma_{HZD}:\begin{cases}\begin{pmatrix}\dot z\\ \dot\alpha_s\end{pmatrix}=\begin{pmatrix}f^*\big|_{Z_{\alpha_s}}(z,\alpha_s)\\ 0\end{pmatrix}, & z^-\notin S_{s\to f}\cap Z_{\blacklozenge}\\ \begin{pmatrix}z^+\\ \alpha_s^+\end{pmatrix}=\begin{pmatrix}\Delta\big|_{S_{s\to f}\cap Z_{\blacklozenge}}(z^-,\alpha_f)\\ \Gamma_s\big|_{S_{s\to f}\cap Z_{\blacklozenge}}(z^-,\alpha_f)\end{pmatrix}, & z^-\in S_{s\to f}\cap Z_{\blacklozenge}\end{cases}. \quad (19)$$

In the general case, inclusion of the inner-loop controller Γ_s is necessary for enforcing conditions (i) and (ii). An example of this situation is the rigid target model controller of Section IV. However, for the SLIP embedding controller of Section V, hybrid invariance can be achieved trivially without the inclusion of the inner-loop controller Γ_s.

A critical aspect of the HZD (19) is its dependence on α_f, which can be selected according to the outer-loop feedback law Γ_f of Fig. 2, intended to exponentially stabilize (19). One way of designing Γ_f is by using discrete LQR techniques. An alternative is to use a modification of Raibert's forward speed controller. Both methods are explored in the following sections.

IV. One DOF Hybrid Zero Dynamics: The Rigid Target Model Controller

This section describes the first of the controllers presented in this paper. The design procedure provides the feedback laws Γ_c, Γ_s and Γ_f, whose function was described in Section III. In this case the procedure results in a one DOF HZD determining the stability of the ASLIP.

A. In-Stride Continuous Control

During the stance phase, the ASLIP exhibits one degree of underactuation. The two inputs $u=(u_1,u_2)'$ will be used to asymptotically impose two virtual holonomic constraints to two DOF, which are chosen to be the leg length and the pitch angle i.e. $q_a=(l,\theta)'$. Other choices are possible; however, this particular one allows for the direct comparison with the SLIP embedding controller of Section V. Here, the virtual constraints are chosen to be polynomials parameterized by the monotonic quantity $q_u=\pi/2-\varphi-\theta$, representing the angle of the leg with respect to the ground, as shown in Fig. 1. The virtual constraints are imposed through zeroing the output

$$y=h(q_s,\alpha_s)=q_a-h_d(q_u,\alpha_s), \quad (20)$$

where h_d are the polynomial functions of q_u describing the desired evolution of q_a, and α_s includes the corresponding polynomial coefficients. Details regarding the polynomial functions are included in the Appendix.

Following the procedure that was outlined in Section III, the continuous feedback controller Γ_c is designed according to (13)-(14), and it renders the surface Z_{α_s} defined by (10) invariant under the flow of the stance dynamics, and attractive. It is emphasized here that *two* virtual holonomic constraints are imposed by zeroing (20), thus resulting in a *one* DOF HZD evolving on a two-dimensional surface Z_{α_s}. This procedure results in the closed-loop hybrid system (15), where, the surface $S_{s\to f}$ is selected to be

$$S_{s\to f}=\{x_s\in TQ_s\mid l-l_0=0,\ \dot l>0\}. \quad (21)$$

To explain (21) note that, when the feedback controller Γ_c is introduced, the liftoff condition becomes a control decision, and is assumed to occur when the leg length obtains a particular value, namely l_0, see also [4].

B. Event-Based Control

The development of the event-based control law closely follows the structure outlined in Section III C. In this case, to achieve the boundary conditions (i) and (ii), it is necessary to include the inner-loop controller Γ_s in the feedback design. Details on how to construct Γ_s are given in the Appendix.

The outer-loop control law Γ_f updates $\alpha_f=(l^{td},\varphi^{td})'$ to exponentially stabilize the HZD. In the rigid target model controller, we do not explore the possibility of updating the touchdown leg length l^{td}; l^{td} is assumed to be always equal to its nominal value l_0. This leaves the touchdown angle φ^{td} as the only parameter available for control. The Poincaré map P associated with (15) under the feedback law Γ_s, gives rise to the discrete-time control system,

$$x_s^-(k+1)=P\big(x_s^-(k),\Gamma_s\big(x_s^-(k),\varphi^{td}(k)\big),\varphi^{td}(k)\big), \quad (22)$$

where $x_s^-(k)$ is the state just prior k-th liftoff. Linearizing (22) and implementing a discrete LQR controller results in

$$\varphi^{td}(k)=\Gamma_f\big(x_s^-(k)\big)=\bar\varphi^{td}+K\big[x_s^-(k)-\bar x_s^-\big], \quad (23)$$

where $\bar x_s^-$ is the nominal value of the state just prior k-th liftoff. The feedback controller (23) guarantees that all the eigenvalues of the linearization of (22) are within the unit circle, and completes the control design. Note that instead of the full model Poincaré map (22), the one-dimensional Poincaré map associated with the HZD (19) could have been used, affording a reduced-order stability test; [13], [4], [7].

V. Two DOF Hybrid Zero Dynamics: The SLIP Embedding Controller

This section describes the second of the controllers

presented in this paper. This controller is fundamentally different from the rigid target model controller of Section IV in that the HZD is *designed* to be a physically compliant dynamic system. As will be shown in Section VI, this has significant implications for perturbation rejection, since it ensures that the *closed-loop* ASLIP behaves like a spring, *even* when it is not on the nominal orbit. This behavior is achieved by designing the HZD to be a "copy" of (i.e. diffeomorphic to) the SLIP hybrid dynamics.

A. In-Stride Continuous Control

In view of the underactuated nature of the stance phase, the control objectives of keeping the torso at a desired constant angle and of the COM evolving according to the SLIP dynamics, will be achieved in different time scales. Since the requirement for the torso being upright throughout the motion is more stringent, high-gain control will be imposed on the pitch rotational motion.

To the continuous part of (6), append the output

$$y = h\left(q_s, \bar{\theta}\right) = \theta - \bar{\theta}, \tag{24}$$

with $\bar{\theta}$ a desired pitch angle. The requirement of $\bar{\theta}$ being constant is a *necessary* condition for matching the ASLIP translational dynamics with the SLIP. The proof of this statement will not be presented here for reasons of space.

Differentiating the output twice results in

$$\frac{d^2 y}{dt^2} = -\frac{L\cos\varphi}{J}u_1 + \frac{L\sin\varphi - l}{Jl}u_2. \tag{25}$$

Equation (25) shows that two inputs are available for zeroing the (single) output (24). In what follows, the hip torque u_2 is solely devoted to pitch control, while the leg input u_1 is reserved for controlling the zero dynamics. This is different from the rigid target model controller, where *no* input was available in the zero dynamics. Since $l \neq L\sin\varphi$ for all the reasonable configurations of the ASLIP, selecting

$$u_2 = \frac{Jl}{L\sin\varphi - l}\left(\upsilon\left(\theta, \dot{\theta}, \varepsilon\right) + \frac{L\cos\varphi}{J}u_1\right) \tag{26}$$

with

$$\upsilon\left(\theta, \dot{\theta}, \varepsilon\right) = -\frac{1}{\varepsilon^2}K_P^\theta\left(\theta - \bar{\theta}\right) - \frac{1}{\varepsilon}K_V^\theta\dot{\theta}, \tag{27}$$

where K_P^θ, K_V^θ are positive constants and $\varepsilon > 0$, renders the zero dynamics surface (10) invariant and attractive. It should be pointed out that, contrary to the rigid target model controller, the zero dynamics surface is a four-dimensional embedded submanifold of the state space TQ_s. This complicates stability analysis of the resulting HZD, which is no longer a one DOF system as was in Section IV.

However, the presence of u_1 in the zero dynamics allows for control action. A feedback law can be devised for u_1 so that the zero dynamics associated with the output (24) matches exactly the differential equations of the SLIP dynamics. Intuitively, if the torso is kept at a constant pitch angle, u_1 can be selected so that the motion of the ASLIP COM is governed by the SLIP dynamics. Formally, this can be achieved by studying (15) under the feedback law (26)-(27) as a singularly perturbed model, with ε being the perturbation parameter. The details of this analysis have been presented in [8], and will not be included here. It is only mentioned that the resulting control law is given by

$$u_1 = \frac{l - L\sin\varphi}{r}F_{\text{SLIP}}, \tag{28}$$

where

$$r = \sqrt{L^2 + l^2 - 2Ll\sin\varphi}, \tag{29}$$

is the distance between the COM and the toe, Fig. 1, and

$$F_{\text{SLIP}} = k\left(r_0 + \Delta r - r\right) + F_E. \tag{30}$$

The last expression (30) can be recognized as the spring force acting along a SLIP leg with stiffness k and uncompressed length $r_0 + \Delta r$ (r_0 is the nominal leg length determining touchdown and Δr is a pretension). The term F_E not present in the classical SLIP corresponds to a corrective force intended to stabilize the total energy of the SLIP at a nominal value $\bar{E}$, and it is given by

$$F_E = -K_P^E\left(\frac{l - L\sin\varphi}{r}\dot{l} - \frac{Ll\cos\varphi}{r}\dot{\varphi}\right)\left(E - \bar{E}\right), \tag{31}$$

where $K_P^E > 0$, and E is the total energy

$$E = \frac{1}{2}m\left(\dot{l}^2 + l^2\dot{\varphi}^2\right) + mg\left(l\cos\left(\varphi + \bar{\theta}\right) + L\sin\bar{\theta}\right) + \frac{1}{2}k\left(r_0 + \Delta r - r\right)^2. \tag{32}$$

This modification is necessary since, in the classical SLIP, perturbations away from the nominal energy cannot be corrected due to the conservative nature of the system.

Combining (26)-(27) and (28)-(32), a feedback controller of the form $u = \Gamma_c\left(x_s, \alpha_s\right)$ is obtained. The vector $\alpha_s = (\bar{\theta}, k, r_0, \Delta r)'$ corresponds to parameters that have been introduced by the control law, and includes the mechanical properties of the target model. These parameters will be selected in Section VI via an optimization procedure. The resulting closed-loop system has the form of (15) with

$$S_{s\to f} = \left\{x_s \in TQ_s \,\middle|\, r_0 - \sqrt{L^2 + l^2 - 2Ll\sin\varphi} = 0\right\}. \tag{33}$$

Intuitively, (33) means that liftoff in the *closed-loop* ASLIP occurs when the distance between the foot and the COM becomes equal to r_0. This assumption is based on the fact that, in the closed-loop system, transition into flight is a control decision, as is explained in [4].

B. Event-Based Control

In deriving an event-based feedback law Γ_s and Γ_f, it is useful to observe that the pitch angle during flight is

governed by trivial dynamics i.e. $\ddot{\theta}=0$. Hence, if liftoff occurs on the zero dynamics i.e. when $\theta^{-}=\bar{\theta}$ and $\dot{\theta}^{-}=0$, then at touchdown we have $\theta^{+}=\bar{\theta}$ and $\dot{\theta}^{+}=0$, i.e. landing occurs on the zero dynamics. Thus, the requirement for hybrid invariance is trivially satisfied. This observation removes the need for an inner-loop controller Γ_{s}.

Next, the outer-loop controller Γ_{f} is designed to exponentially stabilize the ASLIP HZD (19) through the use of available SLIP event-based (touchdown angle) controllers. This is achieved in two levels.

In the first level, conditions ensuring that the reset map of the ASLIP HZD (19) is equal to the SLIP reset map are imposed. Since the translational dynamics of the ASLIP and the SLIP coincide in flight, Γ_{f} is designed so that the flight phase is interrupted at identical conditions in both systems. Hence, if r_0 is the nominal (touchdown) length of the SLIP leg and ψ its touchdown angle, see Fig. 1, the conditions

$$l^{\mathrm{td}}(\psi)=\sqrt{L^2+r_0^2+2Lr_0\sin\left(\psi-\bar{\theta}\right)}\,, \tag{34}$$

$$\varphi^{\mathrm{td}}=\arcsin\left[\frac{\left(l^{\mathrm{td}}\right)^2+L^2-r_0^2}{2Ll^{\mathrm{td}}}\right], \tag{35}$$

ensure that the SLIP touchdown condition is identical to the corresponding one for the ASLIP (2).

In the second level, the angle ψ, see Fig. 1, is updated according to the feedback law,

$$\psi\left(\dot{x}_{\mathrm{c}}^{-}\right)=\bar{\psi}+K_{\dot{x}}\left(\dot{x}_{\mathrm{c}}^{-}-\dot{\bar{x}}_{\mathrm{c}}\right); \tag{36}$$

$\dot{\bar{x}}_{\mathrm{c}}$ and $\bar{\psi}$ are the nominal forward speed and touchdown angle of the SLIP with nominal energy $\bar{E}$, respectively, and $\dot{x}_{\mathrm{c}}^{-}$ is the actual speed of the ASLIP at liftoff. It can be recognized that (36) corresponds to a variation of Raibert's control law, [9]. Control laws similar to (36) exist in the literature, e.g. [2], [11], [12], and they all are equally valid candidates for updating ψ; this particular one has been chosen for illustrative purposes. It is remarked that while the event-based controller (34)-(36) achieves exponential stability of the ASLIP, letting the pitch angle in (34) be equal to its actual value (via continuous feedback during the flight phase), instead of its nominal value $\bar{\theta}$, enlarges the domain of attraction of the controller. This modification will be included in the simulations of Section VI.

VI. Controller Evaluation Via Simulation

A. Nominal Orbit Design Through Optimization

The mechanical properties of the ASLIP used in the simulations correspond to a biped robot currently under construction (see [6] for design details), and are presented in Table I (see also Fig. 1). To implement the rigid target model controller, a sixth order polynomial was used for the desired leg length, and a constant polynomial for the desired pitch angle; see Appendix. Generally, the rigid target model controller allows for the desired θ being any suitably parameterized function of q_u, thus allowing for nontrivial motions of the torso. However, this is not possible in the SLIP embedding controller, due to constant pitch throughout the nominal motion being a necessary condition for its implementation.

TABLE I

SIMULATION PARAMETERS

Parameter	Value	Units
Torso Mass (m)	27	kg
Torso Inertia (J)	1	kg m^2
Hip to COM Spacing (L)	0.25	m
Nominal Leg Length (l_0)	0.9	m
Uncompressed Spring Length (l_{nat})	0.91	m
ASLIP Spring Constant (k_{A})	7578	N/m

Both controllers introduced a set of parameters α_{s}, whose values along the nominal orbit can be selected using the optimization technique developed in [13]. Consider the closed-loop hybrid system (15) with cost function

$$\hat{J}(\alpha_{\mathrm{s}})=\frac{1}{T_{\mathrm{s}}}\int_0^{T_{\mathrm{s}}}u_2^2(t)dt+\max_{t\in[0,T_{\mathrm{s}}]}\left\{\left[u_1(t)-k_{\mathrm{A}}\left(l_{\mathrm{nat}}-l(t)\right)\right]^2\right\}, \tag{37}$$

where T_{s} is the duration of the stance phase, k_{A} is the stiffness of the ASLIP leg, and l_{nat} its natural length, see Table I. Append to (37) the constraint

$$x_{\mathrm{s}}^{-}-P\left(x_{\mathrm{s}}^{-},\alpha_{\mathrm{s}},\alpha_{\mathrm{f}}\right)=0\,, \tag{38}$$

so that the nominal orbit is periodic. One can also include constraints that correspond to requirements such as the desired nominal forward speed, or the normal ground force component be non-negative etc. Then, the problem of finding the nominal values of the coefficients α_{s} and α_{f} reduces to a constrained minimization problem, which can be (numerically) solved using MATLAB's `fmincon`. It worth mentioning here that this choice of performance index reflects our desire to find a nominal orbit for the ASLIP, on which the amount of work produced by the hip actuator and the peak force developed by the leg actuator

$$u_1^a=u_1-k_{\mathrm{A}}\left(l_{\mathrm{nat}}-l\right), \tag{39}$$

are minimized.

B. Steady-State Behavior

In order to compare the behavior of the two controllers under perturbations, it would be ideal to have identical nominal orbits. Using relatively low degree polynomials in the rigid target model controller, an almost exact match in the resulting nominal orbits was obtained, as Fig. 3 presents. Fig. 3 also shows that both controllers take advantage of the leg spring on the nominal (steady-state) motion, since the leg actuator force u_1^a given by (39) is below $6N$ in both cases.

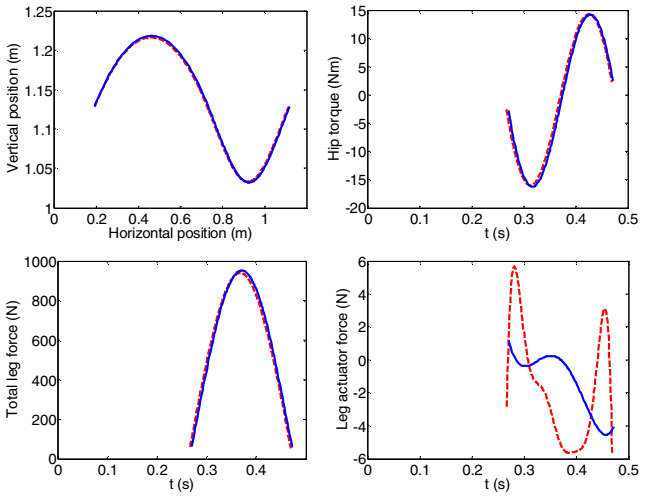

Fig. 3. Nominal orbits and corresponding inputs for the rigid target model controller (dashed lines) and the SLIP embedding controller (solid lines).

C. *Transient Behavior and Performance Evaluation*

The gains used in the rigid target model controller are

$K_P^y = \mathrm{diag}(100,100)$, $K_V^y = 2\sqrt{K_P^y}$, $\varepsilon = 1$, and

$K = (0.1839, 0.4555, -0.0048, 0.0887, 0.1902)$,

while the gains for the SLIP embedding controller are

$K_P^\theta = 300$, $K_V^\theta = 2\sqrt{K_P^\theta}$, $\varepsilon = 1.2$, $K_P^E = 2$, and $K_{\dot{x}} = 0.2$.

Note that K was selected using MATLAB's `dlqr` on the discrete system (22) evolving on the Poincaré section (21).

Both controllers have been simulated in MATLAB. It was observed that the rigid target model controller tends to violate the unilateral ground force constraint by developing control forces which "pull" the ground, even at small perturbations. To enlarge the domain of attraction, it was necessary to include saturation on the control forces so that all the ground constraints are respected. The SLIP embedding controller did not violate these constraints, except at very large perturbations, and hence no input saturation was necessary.

Fig. 4 presents pitch angle and forward velocity as the ASLIP recovers from a perturbation $\delta\theta = -6\,\mathrm{deg}$ using both controllers. The response of the pitch angle is similar; however, larger excursions from the nominal forward speed are observed in the rigid target model controller.

Fig. 5 presents the total leg forces and the leg actuator forces corresponding to Fig. 4. It is seen that, in the SLIP embedding controller, the profile of the leg actuator forces u_1^a computed by (39) remains close to that of a spring force, *even* during transients. On the contrary, in the rigid target model controller, the profile of the total leg force u_1 significantly differs from that of the spring force, resulting in excessively large actuator forces u_1^a. This means that the rigid target model controller in closed loop with the ASLIP effectively "cancels" the compliance of the leg in the open-loop ASLIP. It is emphasized that, on the nominal orbit, both controllers exploit the leg spring equally well, since as shown in Fig. 3, the leg actuator force never exceeds $6N$, while the total forces are on the order of $1000N$.

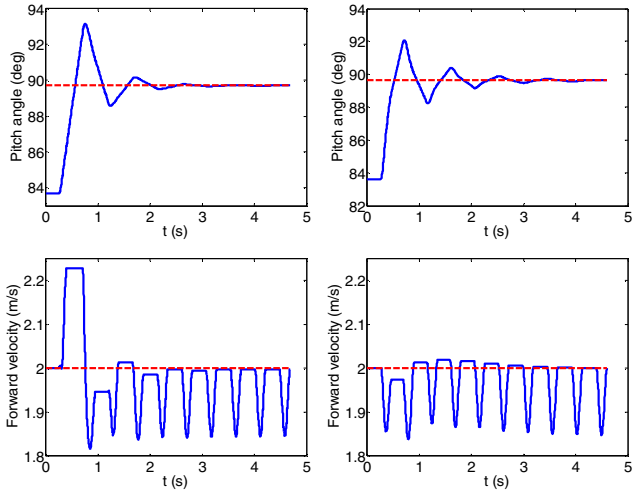

Fig. 4. Ten strides showing convergence from $\delta\theta = -6\,\mathrm{deg}$, for the rigid target model controller (left), and the SLIP embedding controller (right). Dashed lines show desired values.

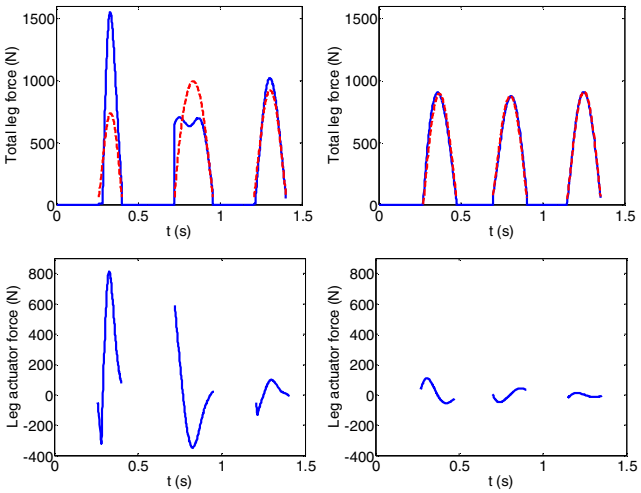

Fig. 5. Leg forces for the rigid target model controller (left) and SLIP embedding controller (right) for the three first steps of Fig. 4. Upper plots show total leg forces; bottom plots show leg actuator forces computed by (39). The dashed lines in the upper plots show spring forces.

These features have significant implications for the domain of attraction of the two controllers. This is demonstrated in Table II, which presents the number of strides until convergence within 5% of the steady-state value (strides), the peak actuator forces $(u_1^a, u_2)^{\max}$ in N, and the total work $(W_1, W_2)^{\mathrm{total}}$ in J, required to reject perturbations $\delta\theta$ in the pitch angle and $\delta\dot{x}_c$ in the forward velocity using the Rigid Target Model controller (RTM) and the SLIP embedding controller (SLIP). The perturbations reported in Table II correspond to the maximum values that can be rejected with the RTM controller, with the leg actuator force satisfying $u_1^a \le 500N$. Larger perturbations than those in Table II can be rejected by the SLIP embedding controller while respecting the constraint $u_1^a \le 500N$. Indeed, as is

shown in Table II, significantly lower peak leg forces and total work are required from the SLIP embedding controller to reject the same perturbations. These results demonstrate the necessity of designing the HZD of running to respect the compliance available in the open-loop system. Otherwise, the beneficial effects of the actual leg spring maybe cancelled by the control inputs during transients.

TABLE II

DOMAIN OF ATTRACTION

Perturbation	Control	Stride	$(u_1^a, u_2)^{\max}$	$(W_1, W_2)^{\text{total}}$
$\delta\theta = +4^o$	RTM	6	$(442,15)$	$(71,24)$
	SLIP	4	$(54,28)$	$(24,18)$
$\delta\theta = -3^o$	RTM	4	$(382,21)$	$(55,19)$
	SLIP	4	$(50,26)$	$(16,19)$
$\delta\dot{x}_c = +0.9\,{}^{\text{m}}/_{\text{s}}$	RTM	12	$(448,37)$	$(242,76)$
	SLIP	6	$(418,64)$	$(110,40)$
$\delta\dot{x}_c = -1.4\,{}^{\text{m}}/_{\text{s}}$	RTM	15	$(486,15)$	$(236,47)$
	SLIP	Cannot reject such a large perturbation without input saturation		

VII. CONCLUSION

In this paper, two controllers, the rigid target model controller and the SLIP embedding controller, are presented for the ASLIP, an extension of the SLIP that includes nontrivial torso pitch dynamics. The control action creates a lower-dimensional hybrid subsystem determining the stability properties of periodic motions of the full model. The rigid target model controller results in a one-degree-of-freedom non-compliant subsystem through imposing suitably parameterized (virtual) holonomic constraints on the ASLIP. The SLIP embedding controller affords a feedback law, under whose influence the SLIP emerges from the ASLIP dynamics, allowing the direct use of a large body of SLIP controllers available in the literature. It is seen through comparisons of the two controllers that the underlying compliant nature of the SLIP enhances performance through significantly improving the transient response. This paper should be viewed as a first step toward a general framework for controller design with compliant hybrid zero dynamics.

APPENDIX

This appendix complements Section IV, and provides details on how to design Γ_c and Γ_s. To ease implementation, it is favorable to use Bézier polynomials. Let $q_u^{\min}$ and $q_u^{\max}$ be the (known) min and max values, respectively, of the angle q_u of the leg with respect to the ground during the *nominal* stance motion, and define $s = (q_u - q_u^{\min})/(q_u^{\max} - q_u^{\min}) \in [0,1]$. Then, the desired leg length parameterized by a Bézier polynomial is given by

$$l_d(s) = \sum_{j=0}^{M} \left[\frac{M!}{j!(M-j)!} s^j (1-s)^{M-j} \right] \alpha_j , \qquad (40)$$

where the coefficients α_j satisfy the following properties

$$l_d(0) = \alpha_0 ,\ l_d(1) = \alpha_M , \qquad (41)$$

$$(\partial l_d / \partial s)\big|_{s=0} = M(\alpha_1 - \alpha_0) ,\ (\partial l_d / \partial s)\big|_{s=1} = M(\alpha_M - \alpha_{M-1}) . \qquad (42)$$

The properties (41) and (42) are exactly those required to ensure conditions (i) and (ii) of Section III C. Suppose that $x_s^- \in S_{s\to f} \cap Z_{\alpha_s}$ and $\alpha_f = (l^{td}, \varphi^{td})'$ is given (specified by the outer-loop feedback law Γ_f). To ensure that the state at touchdown belongs in the zero dynamics surface i.e. $x_s^+ = \Delta(x_s^-, \alpha_f) \in Z_{\alpha_s^+}$, it is sufficient to update the two first coefficients α_0 and α_1 according to

$$\alpha_0^+ = l^+ \text{ and } \alpha_1^+ = \frac{\dot{l}^+}{M\dot{s}} + \alpha_0^+ . \qquad (43)$$

Leaving the rest of the coefficients unchanged (i.e. equal to their nominal values), ensures that $S_{s\to f} \cap Z_{\alpha_s^+} = S_{s\to f} \cap Z_{\alpha_s}$. which is the surface $S_{s\to f} \cap Z_{\blacklozenge}$ in Section III C. Equation (43) provides a rule for updating α_s. The pitch angle polynomial need not be updated due to the trivial pitch dynamics in flight.

REFERENCES

[1] Ahmadi M. and Buehler M., "Controlled Passive Dynamic Running Experiment with the ARL Monopod II," *IEEE Tr. on Robotics*, Vol. 22, No. 5, pp. 974-986, 2006.

[2] Altendorfer R., Koditschek D. E., and Holmes P., "Stability Analysis of Legged Locomotion by Symmetry-Factored Maps," *The Int. J. of Robotics Research*, Vol. 23, No 10-11, pp. 979-1000, 2004.

[3] Cherouvim N., and Papadopoulos E., "Single Actuator Control Analysis of a Planar 3DOF Hopping Robot," S. Thrun, G. Sukhatme, S. Schaal (Eds.), *Robotics: Science and Systems I*, pp. 145-152, MIT Press, Cambridge MA, 2005.

[4] Chevallereau C., Westervelt E., and Grizzle J., "Asymptotically Stable Running for a Five-Link, Four-Actuator, Planar Bipedal Robot," *The Int. J. of Robotics Research*, Vol. 24, No. 6, p. 431–464, 2005.

[5] Full R. J. and Koditschek D., "Templates and Anchors: Neuromechanical Hypotheses of Legged Locomotion on Land," *J. of Exp. Biology*, Vol. 202, pp. 3325-3332, 1999.

[6] Hurst J. W., Chestnutt J. E., and Rizzi A., "Design and Philosophy of the BiMASC, a Highly Dynamic Biped," *Proc. of the IEEE Int. Conf. on Robotics and Automation*, pp. 1863-1868, Roma, Italy, 2007.

[7] Morris B. and Grizzle J. W. "Hybrid Invariance in Bipedal Robots with Series Compliant Actuators," *Proc. of the IEEE Int. Conf. on Decision and Control*, pp. 4793-4800, San Diego, USA, 2006.

[8] Poulakakis I. and Grizzle J., "Formal Embedding of the Spring Loaded Inverted Pendulum in an Asymmetric Hopper," *Proc. of the European Control Conference*, Kos, Greece, 2007.

[9] Raibert M. H., *Legged Robots that Balance*, MIT Press, Cambridge MA, 1986.

[10] Saranli U., and Koditschek D. E., "Template Based Control of Hexapedal Running," *Proc. of the IEEE Int. Conf. on Robotics and Automation*, Vol. 1, pp. 1374-1379, Taipei, Taiwan, 2003.

[11] Schwind W., *Spring Loaded Inverted Pendulum Running: A Plant Model*, PhD Thesis, Univ. of Michigan, Ann Arbor, MI, 1998.

[12] Seyfarth A., Geyer H., Herr H., "Swing leg retraction: A simple control model for stable running," *J. of Exp. Biology*, Vol. 206, pp. 2547-2555, 2003.

[13] Westervelt E.R., Grizzle J.W., and Koditschek D.E., "Hybrid Zero Dynamics of Planar Biped Walkers," *IEEE Tr. on Automatic Control*, Vol. 48, No. 1, pp. 42-56, 2003.